

# Radiosynthesis, In Vitro Validation, and In Vivo Evaluation of $^{18}\text{F}$ -Labeled COX-1 and COX-2 Inhibitors

Timothy J. McCarthy, PhD<sup>1</sup>; Ahmed U. Sheriff, MS<sup>1</sup>; Matthew J. Graneto, BS<sup>2</sup>; John J. Talley, PhD<sup>2</sup>; and Michael J. Welch, PhD<sup>1</sup>

<sup>1</sup>Mallinckrodt Institute of Radiology, Washington University School of Medicine, St. Louis, Missouri; and <sup>2</sup>Discovery Research, Pharmacia Corporation, St. Louis, Missouri

In this article, we describe the radiosynthesis and evaluation of  $^{18}\text{F}$ -labeled cyclooxygenase (COX) inhibitors.  $^{18}\text{F}$ -SC63217 is selective to COX-1 and has a COX-1 inhibitory concentration of 50% ( $\text{IC}_{50}$ ) < 10 nmol/L and a COX-2  $\text{IC}_{50}$  > 100  $\mu\text{mol/L}$ .  $^{18}\text{F}$ -SC58125 has  $\text{IC}_{50}$  values of >100  $\mu\text{mol/L}$  (COX-1) and <86 nmol/L (COX-2). **Methods:** SC63217 and SC58125 were both labeled with  $^{18}\text{F}$  by nucleophilic displacement of a trimethylammonium triflate salt using a dedicated microwave cavity. Each compound was evaluated in vitro using a murine macrophage cell line (J774). COX-2 was stimulated in these cells by treatment with lipopolysaccharide and interferon- $\gamma$ . Both radiotracers were further investigated in vivo using rat biodistribution techniques. Brain uptake of the COX-2 inhibitor,  $^{18}\text{F}$ -SC58125, was further investigated by brain PET of a baboon. **Results:** The in vitro studies showed that uptake of  $^{18}\text{F}$ -SC58125 was increased in stimulated cells and was totally inhibited by the addition of non-radioactive SC58125. In contrast, no increase in uptake was seen for  $^{18}\text{F}$ -SC63217. In the biodistribution experiments,  $^{18}\text{F}$ -SC63217 showed much higher uptake in the small intestine (an organ known to express high levels of COX-1) than did  $^{18}\text{F}$ -SC58125. Higher levels of  $^{18}\text{F}$ -SC58125 were observed in the kidney, an organ known to contain high levels of COX-2 rather than COX-1.  $^{18}\text{F}$ -SC58125 was retained in brain tissue. PET images of the baboon showed no regional distribution of the radiotracer in the brain. **Conclusion:** We have developed a radiosynthetic route that can yield  $^{18}\text{F}$ -labeled selective inhibitors of COX-1 or COX-2. Both compounds have been fully characterized in vitro and in vivo. Our results indicate that  $^{18}\text{F}$ -SC58125 has potential as a marker of COX-2 activity but that, because of high nonspecific binding,  $^{18}\text{F}$ -SC63217 was not a good choice as a marker of COX-1.

**Key Words:** cyclooxygenase; PET;  $^{18}\text{F}$ ; enzyme inhibitors; SC58125; SC63217

J Nucl Med 2002; 43:117–124

Cyclooxygenase (COX) enzymes head a complex biosynthetic cascade that results in the conversion of polyunsaturated fatty acids to prostaglandins and thromboxanes—a family of autocrine and paracrine mediators that contribute to many physiologic and pathophysiologic responses (1).

After the discovery of 2 distinct isoforms of the COX enzyme (2–4), an increased risk of gastrointestinal ulceration was found to be associated with prostaglandins derived from COX-1. Research into the development of inhibitors selective for COX-2 has yielded the 2 approved, highly selective inhibitors, celecoxib (5) and rofecoxib (6), shown in Figure 1. Besides being associated with inflammation, COX-2 induction has been implicated in a number of other processes, including angiogenesis, bone absorption, colon cancer, and altered renal function (7,8).

The motivation for the current study was to develop a positron-labeled selective inhibitor of COX-1 and COX-2 so that their in vitro and in vivo behavior could be studied using PET. Development of selective probes for these 2 enzyme subtypes may help us understand the involvement of the COX pathway in various inflammatory diseases. The candidates that were identified for radiolabeling were a COX-1 selective inhibitor, SC63217, and a COX-2 selective inhibitor, SC58125 (9).

SC63217 has a COX-1 inhibitory concentration of 50% ( $\text{IC}_{50}$ ) < 10 nmol/L and a COX-2  $\text{IC}_{50}$  > 100  $\mu\text{mol/L}$ ; in contrast, SC58125 has  $\text{IC}_{50}$  values of >100  $\mu\text{mol/L}$  (COX-1) and <86 nmol/L (COX-2). Both compounds are structurally similar and differ in the substituents on only 1 aromatic ring (Fig. 2). SC63217 is a derivative of the potent and selective COX-1 inhibitor, SC560 (10), and the structure of SC58125 is closely related to that of celecoxib. The presence of a para-fluoro substituent on both compounds suggested that we might be able to label both compounds with  $^{18}\text{F}$  at a high specific activity.

In this article, we describe the radiolabeling of both inhibitors with  $^{18}\text{F}$ , their initial in vitro evaluation, and their in vivo biodistribution in rats. In addition, we report pre-

Received Apr. 24, 2001; revision accepted Sep. 21, 2001.  
For correspondence or reprints contact: Michael J. Welch, PhD, Division of Radiological Sciences, Washington University School of Medicine, 510 S. Kingshighway Blvd., St. Louis, MO 63110.  
E-mail: welchm@mir.wustl.edu

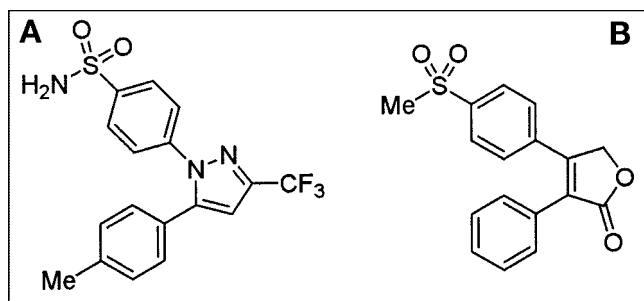


**FIGURE 1.** Structures of celecoxib (A) and rofecoxib (B).

liminary PET findings for the COX-2 inhibitor in a nonhuman primate.

## MATERIALS AND METHODS

Unless otherwise stated, all chemicals were obtained from Aldrich Chemical Co. (Milwaukee, WI). Proton magnetic resonance spectra were obtained on a Gemini 300 spectrometer (Varian, Inc., Palo Alto, CA) at 300 MHz. Chemical shifts are reported in parts per million downfield from tetramethylsilane. The Mass Consortium (San Diego, CA) conducted mass spectral analyses. Materials were heated using a custom-designed (11) microwave cavity, model 420 BX (Resonance Instruments, Skokie, IL). High-performance liquid chromatography (HPLC) was performed on 2 systems. The first was a semipreparative GP50 gradient pump (Dionex Corp., Sunnyvale, CA) equipped with an ultraviolet detector operating at 254 nm (Lambda-Max, model 480; Waters, Milford, MA), a well scintillation NaI(Tl) scintillation detector and associated electronics, and a fraction collector (Microfractionator; Gilson, Inc., Middletown, WI). Samples were eluted through a normal-phase HPLC column (Partisil 10, 50 × 0.94 cm; Whatman, Ann Arbor, MI) with a mixture of 80% hexane and 20% (1:19) isopropanol:dichloromethane at a flow rate of 3 mL/min. The second HPLC system was an analytic gradient pump (GP50; Dionex Corp., Sunnyvale, CA) equipped with an ultraviolet detector operating at 254 nm (Lambda-Max, model 480) and a well scintillation NaI(Tl) scintillation detector and associated electronics. Samples were eluted through a reversed-phase HPLC column (Rocket [Alltima C-18, 3 μm], 53 × 7 mm; Alltech Associates, Inc., Deerfield, IL) with a mixture of 70% acetonitrile and 30% KH<sub>2</sub>PO<sub>4</sub> (0.01 mol/L) at a flow rate of 2 mL/min.

### Preparation of Radiopharmaceutical Precursors

**4,4,4-Trifluoro-1-(p-N,N-Dimethylaminophenyl)-1,3-Butandione (Compound 1).** A solution of sodium ethoxide in ethanol was prepared by dissolving 62.1 mg (2.7 mmol) fresh sodium metal into ethanol (2 mL). To this was added a solution of *p*-N,N-dimethylacetophenone (220 mg, 1.35 mmol) in ethanol (2 mL). After the mixture had been stirred at room temperature for 30 min, ethyltrifluoroacetate (488 μL, 4.1 mmol) was added dropwise. After 1 h, thin-layer chromatography revealed that the reaction was complete. The mixture was diluted into ethyl acetate (50 mL) and filtered through a plug of silica gel. The resultant solution was concentrated in vacuo to furnish 284 mg (81%) of the desired compound, and no further purification was necessary. <sup>1</sup>H nuclear magnetic resonance (NMR) (CDCl<sub>3</sub>) δ-enol form (76%), 7.87 (d, J = 9 Hz, 2H), 6.70 (d, J = 9 Hz, 2H), 6.45 (s, 1H), 3.12 (s, 6H);

keto form (24%), 7.87 (d, J = 9 Hz, 2H), 6.61 (d, J = 9 Hz, 2H), 3.12 (s, 6H), 2.95 (s, 2H).

**1-[4-(Methylsulfonyl)Phenyl]-5-[4,4-(Dimethylaminophenyl)]-3-(Trifluoromethyl)-1H-Pyrazole (Compound 2a).** 4-Methylsulfonylphenylhydrazine (416 mg, 1.87 mmol) was dissolved in ethanol (60 mL) and treated with concentrated hydrochloric acid (1 equivalent, 187 μL). To this solution was added the butadione (440 mg, 1.7 mmol) in ethanol (5 mL). The final solution was heated under reflux for 4 h, after which it was allowed to cool before concentrating. The crude product was purified by silica gel flash column chromatography (50:50 EtOAc:hexane) to yield 416 mg of the desired product as a yellow solid in 55% yield: <sup>1</sup>H NMR (CDCl<sub>3</sub>) δ, 7.94 (d, J = 8.1 Hz, 2H), 7.58 (d, J = 8.1 Hz, 2H), 7.06 (d, J = 9.0 Hz, 2H), 6.67 (s, 1H), 6.64 (d, J = 9.0 Hz, 2H), 3.06 (s, 3H), 3.00 (s, 6H).

**1-(4-Methoxyphenyl)-5-[4,4-(Dimethylaminophenyl)]-3-(Trifluoromethyl)-1H-Pyrazole (Compound 2b).** This compound was prepared by the same method as for compound 2a, except that 4-methoxyphenylhydrazine (1.1 equivalent) was used instead of 4-methylsulfonylphenylhydrazine. The product was isolated by flash column chromatography with an overall yield of 45%. <sup>1</sup>H NMR (CDCl<sub>3</sub>) δ, 7.26 (d, J = 8.1 Hz, 2H), 7.05 (d, J = 8.1 Hz, 2H), 6.86 (d, J = 8.5 Hz, 2H), 6.62 (d, J = 8.5 Hz, 2H), 6.59 (s, 1H), 3.82 (s, 3H), 2.96 (s, 6H).

**1-[4-(Methylsulfonyl)Phenyl]-5-[4,4,4-(Trimethylaminophenyl)]-3-(Trifluoromethyl)-1H-Pyrazole (Trifluoroacetate Salt) (Compound 3a).** To a dry, 10-mL, 2-necked flask under nitrogen was added a solution of the dimethyl pyrazole (compound 2a) (0.12 mmol) in anhydrous dichloromethane (7 mL). The mixture was treated with 1.1 equivalent of methyl triflate (15 μL, 0.13 mmol) and was stirred overnight at room temperature. The mixture was then diluted with ether (10 mL), which precipitated the product as a white powder. This was collected by filtration and used without further purification. <sup>1</sup>H NMR (CD<sub>3</sub>OD) δ, 7.94 (m, 4H), 7.53 (m, 4H), 6.98 (s, 1H), 3.63 (s, 9H), 3.05 (s, 3H). MS [M<sup>+</sup>] 424 (observed); 424.46 (expected).

**1-(4-Methoxyphenyl)-5-[4,4,4-(Trimethylaminophenyl)]-3-(Trifluoromethyl)-1H-Pyrazole (Trifluoroacetate Salt) (Compound 3b).** This triflate salt was prepared by the same method as for compound 3a, except that the pyrazole (compound 2b) was used. <sup>1</sup>H NMR (CD<sub>3</sub>OD) δ, 7.77 (d, J = 9.0 Hz, 2H), 7.43 (d, J = 9.0 Hz, 2H), 7.20 (d, J = 9.3 Hz, 2H), 6.91 (d, J = 9.3 Hz, 2H), 6.80 (s, 1H), 3.81 (s, 3H), 3.70 (s, 9H). MS [M<sup>+</sup>] 376 (observed); 376.16 (expected).

### Preparation of Radiolabeled Materials

**Production of <sup>18</sup>F-Fluoride.** <sup>18</sup>F-Fluoride was produced through proton irradiation (<sup>18</sup>O(p,n)<sup>18</sup>F reaction) of enriched (95%) <sup>18</sup>O-

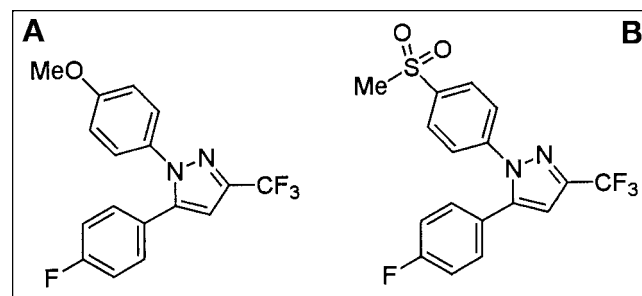


**FIGURE 2.** Structures of SC63217 (A) and SC58125 (B).

water using a JSW BC16/8 cyclotron (The Japan Steel Works, Ltd., Tokyo, Japan) or a CS15 cyclotron (The Cyclotron Corp., Berkeley, CA). Radioactivity emerging from the target was resin treated to reclaim the  $^{18}\text{O}$ -water using the method of Schlyer et al. (12).  $^{18}\text{F}$ -Fluoride was eluted from the resin in a solution of 0.02N potassium carbonate and used in subsequent reactions.

*1-[4-(Methylsulfonyl)Phenyl]-5-(4- $^{18}\text{F}$ -Fluorophenyl)-3-(Trifluoromethyl)-1H-Pyrazole ( $^{18}\text{F}$ -SC58125) (Compound 4a).* To a 5-mL Vacutainer (Becton, Dickinson and Co., Franklin Lakes, NJ) was added 4–5 mg Kryptofix 2.2.2 (Sigma–Aldrich, St. Louis, MO) and 7.4–9.25 GBq (200–250 mCi)  $^{18}\text{F}$ -fluoride (approximately 200–300  $\mu\text{L}$  potassium carbonate solution). Water was azeotropically evaporated from this mixture using HPLC-grade acetonitrile ( $3 \times 0.5\text{ mL}$ ) in an oil bath at  $110^\circ\text{C}$  under a stream of nitrogen.

After the final drying sequence, dimethyl sulfoxide (DMSO) (150  $\mu\text{L}$ ) was added to the residue, and the radioactivity was transferred to a 2-mL Reactivial (Alltech Associates) containing 2 mg of the triflate salt. The Vacutainer was rinsed twice with DMSO (150  $\mu\text{L}$ ), and the washings were added to the Reactivial. The tube was capped firmly, and the contents were briefly mixed before being subjected to microwave irradiation (30 s on medium power) using a custom-designed (11) microwave cavity (Resonance Instruments, Skokie, IL). The contents of the tube were shaken, and the tube was irradiated for a further 15 s and then cooled in a room temperature water bath.

After cooling, the mixture was diluted with water (5 mL) and loaded to a preactivated  $\text{C}_{18}$  SepPak. The cartridge was rinsed with an additional 5 mL water before the radiolabeled products were eluted with ether:pentane (1:3;  $2 \times 5\text{ mL}$ ). The organic layers were passed through a column of magnesium sulfate (approximately 3 g) and collected in a 25-mL round-bottomed flask; after concentration in vacuo, the residue was redissolved in 3 mL hexane: dichloromethane (80:20) and injected onto the semipreparative HPLC system.  $^{18}\text{F}$ -SC58125 (retention time, 29 min) was collected and concentrated before being diluted in dimethylsulfoxide for further studies. The total preparation time was approximately 90 min, with a final non-decay-corrected yield of 10%–20%. A sample of the final product was analyzed by reversed-phase HPLC and determined to be  $>99\%$   $^{18}\text{F}$ -SC58125, with typical specific activities ranging from 37 to 111 GBq/mmol (1,000–3,000 Ci/mmol).

*1-[4-(Methoxyphenyl)]-5-(4- $^{18}\text{F}$ -Fluorophenyl)-3-(Trifluoromethyl)-1H-Pyrazole ( $^{18}\text{F}$ -SC63217) (Compound 4b).* This radio-tracer was prepared in an identical fashion to  $^{18}\text{F}$ -SC58125 and was purified using the same normal-phase HPLC system.  $^{18}\text{F}$ -SC63217 had a retention time of 20 min. Radiochemical purity was  $>99\%$ , and specific activities ranged from 37 to 111 GBq/mmol (1,000–3,000 Ci/mmol).

## In Vitro and In Vivo Radiopharmaceutical Evaluation

*In Vitro Evaluation of  $^{18}\text{F}$ -SC58125 and  $^{18}\text{F}$ -SC63217 in J774 Macrophages.* J774 cells were plated in 6-well plates and grown to confluence in Dulbecco's modified Eagle's medium (DMEM) supplemented with 10% fetal calf serum and 2 mmol/L glutamine. Cells were divided into 4 groups: control, control plus block, pretreated, and pretreated plus block. Two of the groups were pretreated for 18 h with DMEM containing *Escherichia coli* lipopolysaccharide (LPS) (10  $\mu\text{g/mL}$ ) and  $\gamma$ -interferon (50 U/mL); the control groups received DMEM only. Cells were rinsed twice with a modified *N*-(2-hydroxyethyl)piperazine-*N'*-(2-ethanesulfonic

acid) (HEPES)-buffered Krebs solution (131 mmol/L NaCl, 5.5 mmol/L KCl, 1 mmol/L  $\text{MgCl}_2$ , 2.5 mmol/L  $\text{CaCl}_2$ , 25 mmol/L  $\text{NaHCO}_3$ , 1 mmol/L  $\text{NaH}_2\text{PO}_4$ , 5.5 mmol/L D-glucose, 20 mmol/L HEPES, pH 7.4) (13) and maintained at  $37^\circ\text{C}$ . Tracer uptake was initiated by adding approximately 148 kBq (4  $\mu\text{Ci}$ )  $^{18}\text{F}$ -SC58125 or  $^{18}\text{F}$ -SC63217 in DMSO (5  $\mu\text{L}$ ) to each well. For the blocking studies, the tracer was supplemented with a 5  $\mu\text{mol/L}$  solution of corresponding nonradioactive standard. Incubation was terminated at various times by removing the loading buffer from the plates. The monolayers were washed with 2 mL ice-cold phosphate-buffered saline solution 3 times to clear the extracellular spaces and extracted in 2 mL of a solution comprising 1% (w/v) sodium dodecyl sulfate and 10 mmol/L sodium borate. Cell extracts (1 mL) and loading buffer samples (0.1 mL) were counted in an automated well scintillation  $\gamma$ -counter (Gamma 8000; Beckman Coulter, Inc., Fullerton, CA). Cell samples were also measured for protein content using a standard copper reduction/bicinchoninic acid assay, with bovine serum albumin as the protein standard. Uptake data for all experiments were calculated as the percentage of tracer internalized into the cell and normalized for the amount of protein present.

*In Vivo Evaluation of  $^{18}\text{F}$ -SC58125 and  $^{18}\text{F}$ -SC63217.* All animal experiments were conducted under the guidelines established for the care and use of research animals at Washington University.

Biodistribution studies were performed on mature female Sprague–Dawley rats (150–200 g).  $^{18}\text{F}$ -SC58125 or  $^{18}\text{F}$ -SC63217 in dimethylsulfoxide (100  $\mu\text{L}$ ) was administered to the rats under methoxyflurane anesthesia by tail vein injection. For both radio-tracers, blocking studies were conducted in which either SC58125 or SC63217 (10 mg/kg) was coinjected. The animals were allowed free access to food and water. At specific times after administration, the rats were anesthetized again and killed by decapitation. The organs and tissues of interest were removed by dissection and weighed. The radioactivity in each sample was quantified using a Gamma 8000 counter. The percentage injected dose per gram of tissue or organ was calculated by comparison with a weighed and counted sample of the injectate.

PET was performed on a mature female baboon (*Papio anubis*, 17.1 kg, 12 y old) with a 953B PET scanner (CTI, Knoxville, TN/Siemens Medical Systems, Inc., Hoffman Estates, IL) operating in 2-dimensional mode. The reconstructed resolution was approximately 6 mm in the transverse plane and approximately 4.5 mm in the axial direction; axial sampling was approximately 3–4 mm (14). The baboon was anesthetized (ketamine, 15–20 mg/kg; xylazine, 0.25 mg/kg; atropine sulfate, 0.2 mg) before the study began. The plane of anesthesia was maintained throughout the study by additional administration of ketamine (10 mg/kg) as necessary. The animal was placed supine in a U-shaped acrylic holder and was given a continuous intravenous saline drip (400–500 mL total). The head of the baboon was fixed in place by a brace. The head was then positioned with the aid of a vertical line that projected from a laser mounted on the scanner and corresponded to the lowest PET slice when the scanning table was fully advanced into the scanner. A transmission scan of the head was obtained using a  $^{68}\text{Ge}/^{68}\text{Ga}$  rotating rod source. Regional cerebral blood volume was measured using an inhaled bolus of  $^{15}\text{O}$ -carbon monoxide. Regional cerebral blood flow was measured after a bolus injection of  $^{15}\text{O}$ -water. The tracer,  $^{18}\text{F}$ -SC58125 (148 MBq [4 mCi]), was injected intravenously, and images were acquired for 2 h after injection.



## RESULTS

### Chemistry

Both SC63217 and SC58125 were radiolabeled with  $^{18}\text{F}$  by direct nucleophilic displacement of the corresponding trimethylammonium triflate using  $^{18}\text{F}$ -fluoride. Our initial report (15) on these ligands used a fluoro-for-nitro exchange reaction for radiolabeling. For unexplained reasons, this reaction proved unreliable, and as a result, we switched our radiosynthetic strategy to fluoride displacement of a trimethylammonium triflate salt (16).

The construction method for the 1,5-diarylpyrazoles was based on that previously reported (5) for compounds of this type (Fig. 3). The intermediate 1,3-dicarbonyl compound (compound 1) was prepared by Claisen condensation of *p*-dimethylaminoacetophenone with ethyltrifluoroacetate, and the 1,5-diarylpyrazoles (compounds 2a and 2b) were formed by condensation with the appropriate phenylhydrazine salt. Treatment of these products with methyl triflate produced the desired trimethylammonium triflate salts (compounds 3a and 3b) for radiolabeling with  $^{18}\text{F}$ . The salts were radiolabeled in a single step using a dedicated microwave cavity (11).

Radiochemical yields for the final step ranged from 10% to 20%. Losses of radioactivity were attributed to formation of a radiolabeled side product,  $^{18}\text{F}$ -methyl fluoride, formed from nucleophilic attack of the fluoride onto a methyl group of the trimethylammonium triflate (17,18). The ring systems of both the precursor com-

pounds are not significantly activated to nucleophilic displacement by  $^{18}\text{F}$ -fluoride.

### Cell Uptake Studies

The murine macrophage (J774) cell line was used to probe the uptake of both radiotracers in vitro. Pretreating the cells with a mixture of LPS and  $\gamma$ -interferon ( $\text{IFN}\gamma$ ) for 18 h is known to stimulate COX-2 expression (19,20). Both radiotracers were tested in stimulated and nonstimulated J774 cells. The specificity of the radiotracer for either COX-1 or COX-2 was tested by a second set of experiments using the corresponding tracer containing 5  $\mu\text{mol/L}$  SC58125 or SC63217.

Uptake was measured in triplicate for 2 h. The data are represented as the percentage of radiotracer taken into the cell and normalized to the amount of protein present. The results for  $^{18}\text{F}$ -SC58125 are summarized in Fig. 4, and the results for  $^{18}\text{F}$ -SC63217 are summarized in Fig. 5.

### $^{18}\text{F}$ -SC58125 Uptake Data

**Control Cells.** Analysis of the cell uptake data for  $^{18}\text{F}$ -SC58125 revealed moderate accumulation of radioactivity in the cells during the experiment (2 h). When the cells were coincubated with 5  $\mu\text{mol/L}$  SC58125, the uptake was reduced, suggesting a baseline expression of COX-2 in these nonstimulated macrophages.

**LPS/ $\text{IFN}\gamma$ -Stimulated Cells.** In contrast to the control experiment, a much greater uptake of  $^{18}\text{F}$ -SC58125 was observed in the stimulated cells over 2 h. This uptake could

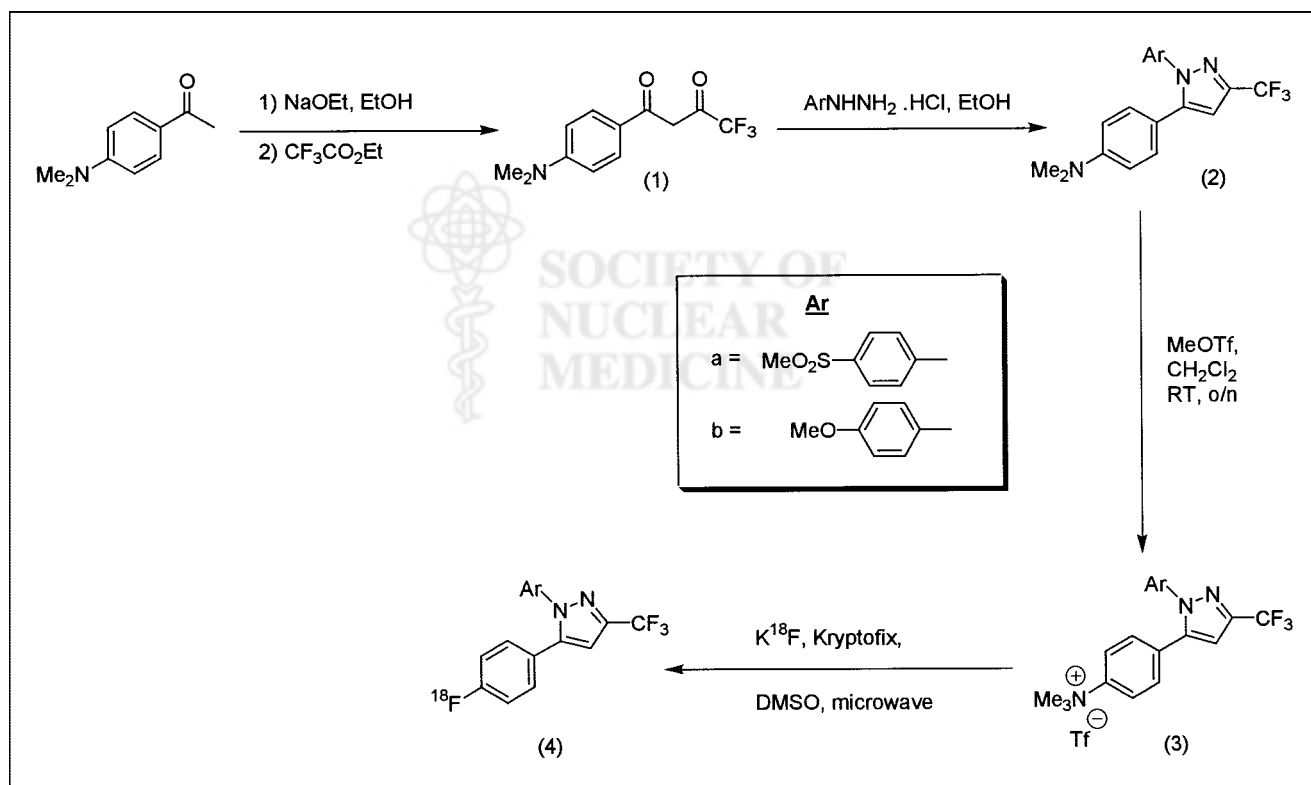


**FIGURE 3.** Synthesis and radiosynthesis of  $^{18}\text{F}$ -SC58125 (compound 4a) and  $^{18}\text{F}$ -SC63217 (compound 4b).

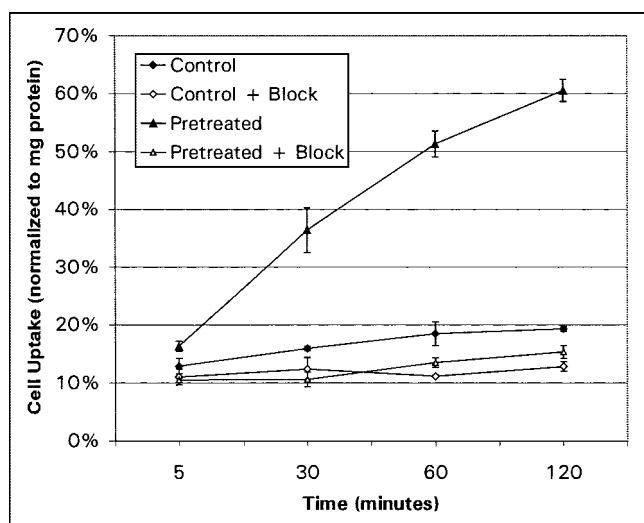


**FIGURE 4.** In vitro study on accumulation of  $^{18}\text{F}$ -SC58125 in J774 macrophage cells. Results are shown as mean  $\pm$  SD ( $n = 3$ ).

be totally inhibited by coincubation with 5  $\mu\text{mol/L}$  SC58125. The blocking effect reduced uptake to levels similar to those of the control cells blocked with SC58125. We have independently confirmed increased expression of COX-2 in this model using Western blot techniques similar to those described for inducible nitric oxide synthase (21). These observations suggest that the increased uptake of  $^{18}\text{F}$ -SC58125 is caused by increased COX-2 expression in the macrophages.

#### $^{18}\text{F}$ -SC63217 Uptake Data

**Control Cells.** The experiments described above were repeated for the COX-1 selective inhibitor. Uptake of the radiotracer over 2 h was observed and could be marginally inhibited by incubation with 5  $\mu\text{mol/L}$  SC63217. These observations suggest that some specific binding to COX-1 was present but that this tracer had a significant level of nonspecific binding.

**LPS/IFN $\gamma$ -Stimulated Cells.** In contrast to our observations with  $^{18}\text{F}$ -SC58125 in stimulated cells, no increased uptake of  $^{18}\text{F}$ -SC63217 was observed when these cells were stimulated with LPS and IFN $\gamma$ . We still observed the high levels of nonspecific binding that were seen for the control experiment with  $^{18}\text{F}$ -SC63217. Because no significant increase in uptake was seen for  $^{18}\text{F}$ -SC63217, we believe that these observations show that SC63217 has no significant affinity to COX-2.

In summary, our in vitro data show that  $^{18}\text{F}$ -SC58125 can detect COX-2 levels in stimulated macrophages. This radiotracer, in contrast to the COX-1 selective radiotracer, appears to have less nonspecific binding, as shown by the lower accumulation of tracer when coincubated with non-radioactive SC58125.

#### Biodistribution Studies

The in vivo biodistribution of both radiotracers in healthy, mature female Sprague-Dawley rats was inves-

tigated. Four time points, ranging from 30 min to 3 h after injection, were examined. The data for the COX-1 inhibitor,  $^{18}\text{F}$ -SC63217, are shown in Table 1, and those for the COX-2 inhibitor,  $^{18}\text{F}$ -SC58125, are shown in Table 2.

Both compounds quickly cleared from the blood pool and showed little uptake by bone, indicating stability to in vivo defluorination. Much higher levels of retention in the small intestine were observed for  $^{18}\text{F}$ -SC63217 than for  $^{18}\text{F}$ -SC58125. We attribute this finding to the high levels of COX-1 that are known to be present in the tissues of the small intestine. The kidney showed higher levels of accumulation for SC58125. COX-2 is known to be strongly expressed in the normal kidney (22), especially in the macula densa, and our data suggest that this accumulation indicates the higher levels of COX-2 present in this tissue. Attempts to block uptake in these tissues by coinjection with nonradioactive SC58125 or SC63217 proved unsuccessful.  $^{18}\text{F}$ -SC63217 did not significantly penetrate the blood-brain barrier; in contrast, the brain retained radioactivity from  $^{18}\text{F}$ -SC58125 until 3 h after injection.

#### Nonhuman Primate PET

We were intrigued by the retention of  $^{18}\text{F}$ -SC58125 in the rat brain and decided to probe this finding using PET of a baboon. Sample images are shown in Figure 6. The first set represents a summed image from immediately to 30 min after injection. Delineation of the brain during this time is caused by radioactivity that has not yet cleared the blood pool. In contrast, the second set of images cover data acquired 1–2 h after injection and delineates radioactivity that has penetrated the blood-brain barrier. No localization of radioactivity was observed within the brain, but we were interested by the appearance of the regions immediately beneath the base of the brain. We believe that this appear-

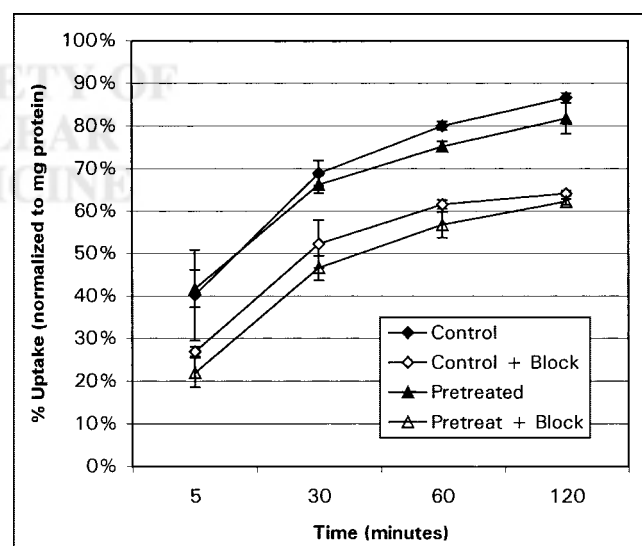


**FIGURE 5.** In vitro study on accumulation of  $^{18}\text{F}$ -SC63217 in J774 macrophage cells. Results are shown as mean  $\pm$  SD ( $n = 3$ ).

**TABLE 1**  
Biodistribution of  $^{18}\text{F}$ -SC63217 in Mature Female Sprague–Dawley Rats

Tissue/organ	Mean percentage injected dose per gram $\pm$ SD			
	30 min ( $n = 3$ )	1 h ( $n = 3$ )	2 h ( $n = 4$ )	3 h ( $n = 3$ )
Blood	$0.04 \pm 0.02$	$0.03 \pm 0.00$	$0.01 \pm 0.01$	$0.02 \pm 0.01$
Lung	$0.27 \pm 0.13$	$0.18 \pm 0.00$	$0.13 \pm 0.02$	$0.13 \pm 0.01$
Liver	$0.35 \pm 0.19$	$0.24 \pm 0.02$	$0.14 \pm 0.03$	$0.23 \pm 0.06$
Kidney	$0.30 \pm 0.06$	$0.17 \pm 0.01$	$0.12 \pm 0.06$	$0.12 \pm 0.03$
Muscle	$0.14 \pm 0.07$	$0.12 \pm 0.02$	$0.09 \pm 0.02$	$0.10 \pm 0.03$
Heart	$0.21 \pm 0.07$	$0.12 \pm 0.01$	$0.06 \pm 0.03$	$0.05 \pm 0.01$
Brain	$0.16 \pm 0.06$	$0.08 \pm 0.01$	$0.02 \pm 0.00$	$0.02 \pm 0.00$
Bone	$0.22 \pm 0.16$	$0.23 \pm 0.03$	$0.17 \pm 0.06$	$0.22 \pm 0.03$
Stomach	$0.06 \pm 0.03$	$0.09 \pm 0.01$	$0.03 \pm 0.01$	$0.03 \pm 0.01$
Small intestine	$4.93 \pm 2.20$	$3.67 \pm 0.84$	$1.28 \pm 0.53$	$2.25 \pm 0.23$

ance was caused by nonspecific uptake of the radiotracer and was associated with structures in the region of the clivus. Interestingly, a similar pattern of distribution was observed by Enas et al. (23) for a high-affinity  $\alpha_2$ -adrenergic antagonist,  $^{18}\text{F}$ -RS-15383-FP.

## DISCUSSION

The radiosynthesis of the 2 compounds proceeded in reasonable yield, considering that neither is particularly activated to nucleophilic displacement by fluoride ion. Use of the microwave cavity facilitated this incorporation; conventional heating of the sample in DMSO at  $130^\circ\text{C}$  for prolonged periods (30–40 min) yielded only low incorporations (1%–2%). We have attempted to monitor the temperature achieved inside the cavity under these conditions, and our estimates put the temperature of the DMSO in excess of  $150^\circ\text{C}$ ; we postulate that a superheating effect of the solvent may be contributing to the increased yields of incorporation. No  $^{18}\text{F}$ -fluoro-for- $^{19}\text{F}$ -fluoro exchange products were observed in the reaction mixture.

The in vitro binding studies of the 2 radiopharmaceuticals in J774 macrophages allowed us to determine if uptake of our COX-2 selective inhibitor, SC58125, was increased as a result of COX-2 stimulation. Incubation of macrophages with LPS is

known to activate several inflammatory cascade mechanisms, the initial steps in this process being binding of LPS to LPS binding protein, with subsequent binding of this complex to the CD14 receptor on the cell surface (24). In our experiments with  $^{18}\text{F}$ -SC58125, we saw increased uptake of the tracer, compared with the uptake in control cells. This uptake could be completely blocked by coincubation with  $5\text{ }\mu\text{mol/L}$  SC58125, suggesting that the increased uptake reflected increased levels of COX-2 expression in the macrophages. Interestingly, the uptake of  $^{18}\text{F}$ -SC58125 in the control cells could be partially blocked by coincubation with  $5\text{ }\mu\text{mol/L}$  SC58125, suggesting that a low baseline level of COX-2 is expressed in the non-stimulated macrophages.

The COX-1 selective inhibitor,  $^{18}\text{F}$ -SC63217, when compared with  $^{18}\text{F}$ -SC58125, showed a much higher level of nonselective binding in J774 cells. However, uptake was not significantly enhanced after stimulation with LPS and IF $\gamma$ —a finding consistent with the lack of significant affinity of SC63217 for the COX-2 enzyme.

The rat biodistribution experiments yielded some interesting results. In the small intestine, uptake of the COX-1 inhibitor was significantly higher than that of the COX-2 inhibitor. We attribute this difference to the higher levels of COX-1 found in that organ. Unfortunately, we were unable

**TABLE 2**  
Biodistribution of  $^{18}\text{F}$ -SC58125 in Mature Female Sprague–Dawley Rats

Tissue/organ	Percentage injected dose per gram $\pm$ SD			
	30 min ( $n = 4$ )	1 h ( $n = 3$ )	2 h ( $n = 4$ )	3 h ( $n = 4$ )
Blood	$0.11 \pm 0.00$	$0.09 \pm 0.01$	$0.07 \pm 0.01$	$0.08 \pm 0.01$
Lung	$0.52 \pm 0.09$	$0.41 \pm 0.01$	$0.34 \pm 0.07$	$0.38 \pm 0.07$
Liver	$1.82 \pm 0.32$	$1.47 \pm 0.06$	$1.22 \pm 0.11$	$1.38 \pm 0.18$
Spleen	$0.26 \pm 0.04$	$0.21 \pm 0.02$	$0.19 \pm 0.03$	$0.20 \pm 0.03$
Kidney	$0.60 \pm 0.09$	$0.46 \pm 0.03$	$0.41 \pm 0.05$	$0.45 \pm 0.08$
Muscle	$0.39 \pm 0.07$	$0.32 \pm 0.06$	$0.34 \pm 0.04$	$0.38 \pm 0.06$
Heart	$0.53 \pm 0.09$	$0.40 \pm 0.03$	$0.35 \pm 0.05$	$0.37 \pm 0.04$
Brain	$0.35 \pm 0.07$	$0.25 \pm 0.00$	$0.25 \pm 0.02$	$0.25 \pm 0.04$
Bone	$0.22 \pm 0.05$	$0.17 \pm 0.02$	$0.15 \pm 0.03$	$0.14 \pm 0.03$
Stomach	$0.21 \pm 0.04$	$0.17 \pm 0.05$	$0.11 \pm 0.02$	$0.13 \pm 0.02$
Small intestine	$0.74 \pm 0.10$	$0.58 \pm 0.07$	$0.38 \pm 0.14$	$0.53 \pm 0.03$

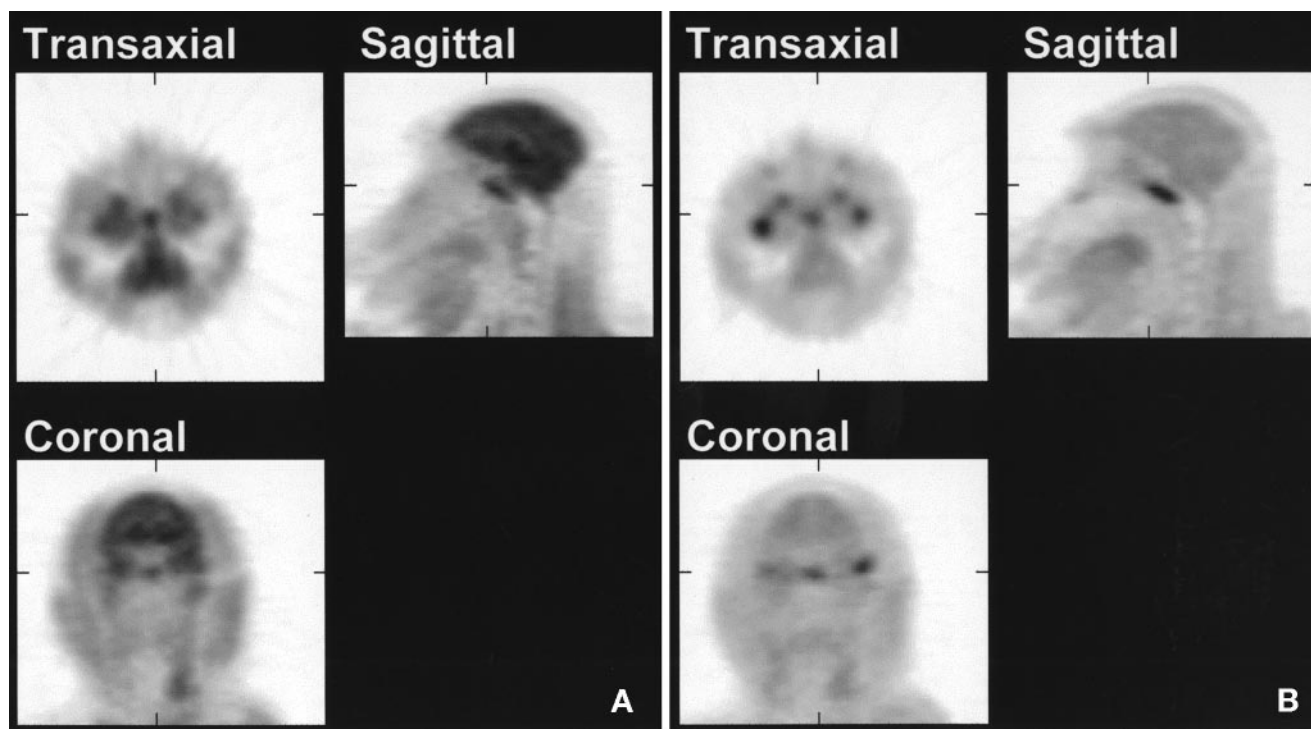


**FIGURE 6.** Sample PET images obtained from injection of  $^{18}\text{F}$ -SC58125 into mature female baboon. (A) Summed images over first 30 min after injection. (B) Summed images from 1 to 2 h after injection.

to obtain any statistically significant blocking data to clearly show that we were truly targeting the enzymes in question. We made similar observations when evaluating a nitric oxide synthase inhibitor,  $^{18}\text{F}$ -5-2-fluoroethylisothiourea (21); at the time, we attributed this problem to a pressor effect exerted by the blocking dose of the ethylisothiourea. In the current example, we believe that the phenomenon is related to pharmacologic effects associated with the blocking dose, but the exact mechanism remains to be determined. Other investigators have observed similar problems for different receptor-based radiopharmaceuticals. For example, Skaddan et al. (25,26) observed that acetylcholinesterase inhibition actually increased the in vivo binding of *N*-(2- $^{18}\text{F}$ -fluoroethyl)-4-piperidyl benzilate to muscarinic acetylcholine receptors.

The relatively high retention of the COX-2 selective inhibitor,  $^{18}\text{F}$ -SC58125, in the rat brain prompted us to study a baboon with PET. Other investigators (27,28) have shown that COX-2 immunoreactive staining of brain slices closely corresponds to COX-2 messenger RNA immunostaining and is enriched in forebrain neurons, particularly in the neocortex, hippocampus, amygdala, and limbic cortices. PET of the baboon brain did not yield any structural information on distribution of the radiotracer that would be consistent with the known immunohistochemistry of COX-2.

## CONCLUSION

In this article, we have reported the radiosynthesis and an initial comparison of 2  $^{18}\text{F}$ -radiolabeled COX inhibitors:

$^{18}\text{F}$ -SC63217 (COX-1 selective) and  $^{18}\text{F}$ -SC58125 (COX-2 selective). Both compounds have been fully characterized in vitro and in vivo. Our in vitro results indicate that  $^{18}\text{F}$ -SC58125 has potential as a marker of COX-2 activity but that, because of high nonspecific binding,  $^{18}\text{F}$ -SC63217 was not a good choice as a marker of COX-1. An in vivo evaluation of both ligands showed that each tracer has a biodistribution compatible with the known distribution of the enzymes.

## ACKNOWLEDGMENTS

The authors thank Jian Wang, Elizabeth Sherman, and Lennis Lich for assistance with the in vitro validation, biodistribution, and baboon imaging studies; P. Duffy Cutler, PhD, and Avi Snyder, MD, for reconstruction and analysis of the PET data; Vallabhaneni Rao, PhD, for Western blot analyses; and Frank Wüst, PhD, for helpful discussions. This study was supported by grant PO1 HL-13851 from the National Institutes of Health and was presented in part at the 42nd annual meeting of the Society of Nuclear Medicine, Minneapolis, MN, June 1995.

## REFERENCES

1. Marnett LJ, Kalgutkar AS. Cyclooxygenase 2 inhibitors: discovery, selectivity and the future. *Trends Pharmacol Sci.* 1999;20:465–469.
2. Kujubu DA, Fletcher BS, Varnum BC, Lim RW, Herschman HR. TIS10, a phorbol ester tumor promoter-inducible mRNA from Swiss 3T3 cells, encodes a novel prostaglandin synthase/cyclooxygenase homologue. *J Biol Chem.* 1991; 266:12866–12872.
3. Xie WL, Chipman JG, Robertson DL, Erikson RL, Simmons DL. Expression of a mitogen-responsive gene encoding prostaglandin synthase is regulated by mRNA splicing. *Proc Natl Acad Sci USA.* 1991;88:2692–2696.



4. O'Banion MK, Sadowski HB, Winn V, Young DA. A serum- and glucocorticoid-regulated 4-kilobase mRNA encodes a cyclooxygenase-related protein. *J Biol Chem*. 1991;266:23261–23267.
5. Penning TD, Talley JJ, Bertenshaw SR, et al. Synthesis and biological evaluation of the 1,5-diarylpyrazole class of cyclooxygenase-2 inhibitors: identification of 4-[5-(4-methylphenyl)-3-(trifluoromethyl)-1H-pyrazol-1-yl]benzenesulfonamide (SC-58635, celecoxib). *J Med Chem*. 1997;40:1347–1365.
6. Prasit P, Wang Z, Brideau C, et al. The discovery of rofecoxib, [MK 966, Vioxx, 4-(4'-methylsulfonylphenyl)-3-phenyl-2(5H)-furanone], an orally active cyclooxygenase-2-inhibitor. *Bioorg Med Chem Lett*. 1999;9:1773–1778.
7. Smith WL, DeWitt DL, Garavito RM. Cyclooxygenases: structural, cellular, and molecular biology. *Ann Rev Biochem*. 2000;69:145–182.
8. Katori M, Majima M. Cyclooxygenase-2: its rich diversity of roles and possible application of its selective inhibitors. *Ann Rev Biochem*. 2000;49:367–392.
9. Talley JJ, Penning TD, Collins PW, et al., inventors; G.D. Searle and Co., assignee. *Substituted pyrazolyl benzenesulfonamides*. U.S. patent 5,466,823. November 14, 1995.
10. Smith CJ, Zhang Y, Koboldt CM, et al. Pharmacological analysis of cyclooxygenase-1 in inflammation. *Proc Natl Acad Sci USA*. 1998;95:13313–13318.
11. Dence CS, Mishani E, McCarthy TJ, Welch MJ. Evaluation of a microwave cavity for the synthesis of PET radiopharmaceuticals. *J Label Compound Radiopharm*. 1995;37:115–117.
12. Schlyer DJ, Bastos MAV, Alexoff D, Wolf AP. Separation of [<sup>18</sup>F]fluoride from [<sup>18</sup>O]water using anion exchange resin. *Appl Radiat Isot*. 1990;41:531–533.
13. Baydoun AR, Mann GE. Selective targeting of nitric oxide synthase inhibitors to system  $\gamma^+$  in activated macrophages. *Biochem Biophys Res Commun*. 1994;200:726–731.
14. Spinks TJ, Jones T, Bailey DL, et al. Physical performance of a positron tomograph for brain imaging with retractable septa. *Phys Med Biol*. 1992;37:1637–1655.
15. McCarthy TJ, Sherman ELC, Talley JJ, Seibert K, Isakson PC. Radiosynthesis, biodistribution and PET imaging of potent and selective inhibitors of cyclooxygenase-1 and cyclooxygenase-2 [abstract]. *J Nucl Med*. 1995;36(suppl):49P.
16. Haka MS, Kilbourn MR, Watkins GL, Toorongian SA. Aryltrimethylammonium trifluoromethanesulfonates as precursors to aryl [<sup>18</sup>F]fluorides: improved synthesis of [<sup>18</sup>F]GBR-13119. *J Label Compound Radiopharm*. 1988;27:823–833.
17. Banks WR, Satter MR, Hwang D-R. A new method for the nca production of [<sup>18</sup>F]fluoromethane. *Appl Radiat Isot*. 1994;45:69–74.
18. Liu N, Ding YS. Is trialkylammonium leaving group always desirable for nucleophilic aromatic substitution reactions with [<sup>18</sup>F]fluoride?: synthesis of [<sup>18</sup>F]-labeled ABT-594 analog. *J Label Compound Radiopharm*. 1999;42(suppl):S555–S557.
19. Riese J, Hoff T, Nordhoff A, Dewitt DL, Resch K, Kaever V. Transient expression of prostaglandin endoperoxide synthase-2 during mouse macrophage activation. *J Leukocyte Biol*. 1994;55:476–482.
20. Pang L, Hoult JR. Induction of cyclooxygenase and nitric oxide synthase in endotoxin-activated J774 macrophages is differentially regulated by indomethacin: enhanced cyclooxygenase-2 protein expression but reduction of inducible nitric oxide synthase. *Eur J Pharmacol*. 1996;317:151–155.
21. Zhang J, McCarthy TJ, Moore WM, Currie MG, Welch MJ. Synthesis and evaluation of two positron labeled nitric oxide synthase inhibitors, S-[<sup>11</sup>C]methylisothiourea and S-(2-[<sup>18</sup>F]fluoroethyl)isothiourea, as potential positron emission tomography tracers. *J Med Chem*. 1996;39:5110–5118.
22. Harris RC. Cyclooxygenase-2 in the kidney. *J Am Soc Nephrol*. 2000;11:2387–2394.
23. Enas JD, Clark RD, VanBroeklin HF. Synthesis and biological evaluation of [F-18]RS-15385-FPh: a potent and selective  $\alpha$ -2 adrenergic receptor ligand. *J Label Compound Radiopharm*. 1997;40:628–630.
24. Guha M, Mackman N. LPS induction of gene expression in human monocytes. *Cell Signal*. 2001;13:85–94.
25. Skaddan MB, Kilbourn MR, Snyder SE, Sherman PS, Desmond TJ, Frey KA. Synthesis, <sup>18</sup>F-labeling, and biological evaluation of piperidyl and pyrrolidyl benzilates as in vivo ligands for muscarinic acetylcholine receptors. *J Med Chem*. 2000;43:4552–4562.
26. Skaddan MB, Kilbourn MR, Snyder SE, Sherman PS. Acetylcholinesterase inhibition increases in vivo N-(2-[<sup>18</sup>F]fluoroethyl)-4-piperidyl benzilate binding to muscarinic acetylcholine receptors. *J Cereb Blood Flow Metab*. 2001;21:144–148.
27. Kaufmann WE, Andreasson KI, Isakson PC, Worley PF. Cyclooxygenase and the central nervous system. *Prostaglandins*. 1997;54:601–624.
28. Breder CD. Cyclooxygenase systems in the mammalian brain. *Ann NY Acad Sci*. 1997;813:296–301.







The Journal of  
NUCLEAR MEDICINE

## Radiosynthesis, In Vitro Validation, and In Vivo Evaluation of $^{18}\text{F}$ -Labeled COX-1 and COX-2 Inhibitors

Timothy J. McCarthy, Ahmed U. Sheriff, Matthew J. Graneto, John J. Talley and Michael J. Welch

*J Nucl Med.* 2002;43:117-124.

---

This article and updated information are available at:  
<http://jnm.snmjournals.org/content/43/1/117>

---

Information about reproducing figures, tables, or other portions of this article can be found online at:  
<http://jnm.snmjournals.org/site/misc/permission.xhtml>

Information about subscriptions to JNM can be found at:  
<http://jnm.snmjournals.org/site/subscriptions/online.xhtml>

*The Journal of Nuclear Medicine* is published monthly.  
SNMMI | Society of Nuclear Medicine and Molecular Imaging  
1850 Samuel Morse Drive, Reston, VA 20190.  
(Print ISSN: 0161-5505, Online ISSN: 2159-662X)

© Copyright 2002 SNMMI; all rights reserved.

 SOCIETY OF  
NUCLEAR MEDICINE  
AND MOLECULAR IMAGING